

Microstructure and properties of lithium and antimony modified potassium sodium niobate lead-free piezoelectric ceramics

Yong SUN,* Dingquan XIAO,*[†] Lang WU,** Dunmin LIN,* Jianguo ZHU,* Ping YU,* Xiang LI,*
Yuanyu WANG,* Yan LI,** Yanzheng LIN,** Yan ZHUANG*** and Qun WEI***

*School of Material Science and Engineering, Sichuan University, Chengdu 610064, China

**School of Material Science and Engineering, Southwest University of Science and Technology,
Mianyang 621010, Sichuan, China

***GCI Science & Technology Co., Ltd., Guangzhou 510310, China

$(\text{K}_{0.52}\text{Na}_{0.48})_{1-x}\text{Li}_x(\text{Nb}_{1-x}\text{Sb}_x)\text{O}_3$ lead-free ceramics were prepared by solid state reaction and the electrical properties of the ceramics were characterized. The crystalline phases and microstructure of the ceramics exhibit much dependence on the content of x , and the orthorhombic and tetragonal phases of the samples coexisted in the composition range of $0.04 \leq x \leq 0.05$ at room temperature. The ceramics with $x = 0.05$ show the better die-, piezo- and ferroelectric properties: piezoelectric constant $d_{33} = 303$ pC/N, planar electromechanical coupling coefficient $k_p = 0.50$, the relative dielectric constant $K = 1228$, synton impedance $R_r = 66.1\Omega$, remnant polarization $P_r = 31.2 \mu\text{C}/\text{cm}^2$, and coercive field $E_c = 0.770$ kV/mm.

©2008 The Ceramic Society of Japan. All rights reserved.

Key-words : Piezoelectric ceramics, Lead-free, Microstructure, Electrical properties

[Received November 15, 2007; Accepted February 21, 2008]

1. Introduction

The most successful piezoelectric ceramics are based on lead zirconate and lead titanate. Environmental concerns over their lead content could disappear with the advent of a new ceramic that is lead-free.¹⁾ Potassium-sodium niobium (KNN)-based lead-free piezoelectric ceramics, the promising candidates for PZT counterparts, has been paid much attention by many specialists in the world especially since 2004.²⁾ However, pure KNN ($\text{K}_{0.5}\text{Na}_{0.5}\text{NbO}_3$) ceramics show relatively lower electrical properties (the piezoelectric constant $d_{33} \sim 80$ pC/N, and the planar electromechanical coupling factor $k_p \sim 36\%$) due to difficulty in the processing of dense ceramics by ordinary sintering.^{3,4)} For the sake of obtaining better electrical performance of the ceramics, lots of routine and unfamiliar approaches have been attempted.⁵⁻⁸⁾ However, the electrical properties of ceramics were not significantly improved by routine approaches, and that unfamiliar ones suffered from the high cost of equipment and from low yield.

Recently with the development of processing techniques, preferable properties, for instance^{9,10)} $d_{33} \sim 314\text{--}328$ pC/N, and $k_p \sim 48\%$, of KNN-based piezoelectric ceramics have been prepared by conventional methods in the labs. It was noticeable that most researchers^{2,5,11-15)} focused their attention on preparing KNN-based ceramics with 0.5/0.5 K/Na ratio and Na rich compositions. Nevertheless, there were few studies on the preparation of lithium and antimony modified KNN lead-free piezoelectric ceramics with K rich compositions. It is well known that the loss of potassium were much higher than sodium's at high temperature, K rich compositions could compensate this kind of loss. It was also intrigued by the phase diagram¹⁶⁾ of $\text{NaNbO}_3\text{--KNbO}_3$ system. Therefore, in this work the K/Na ratio was changed from

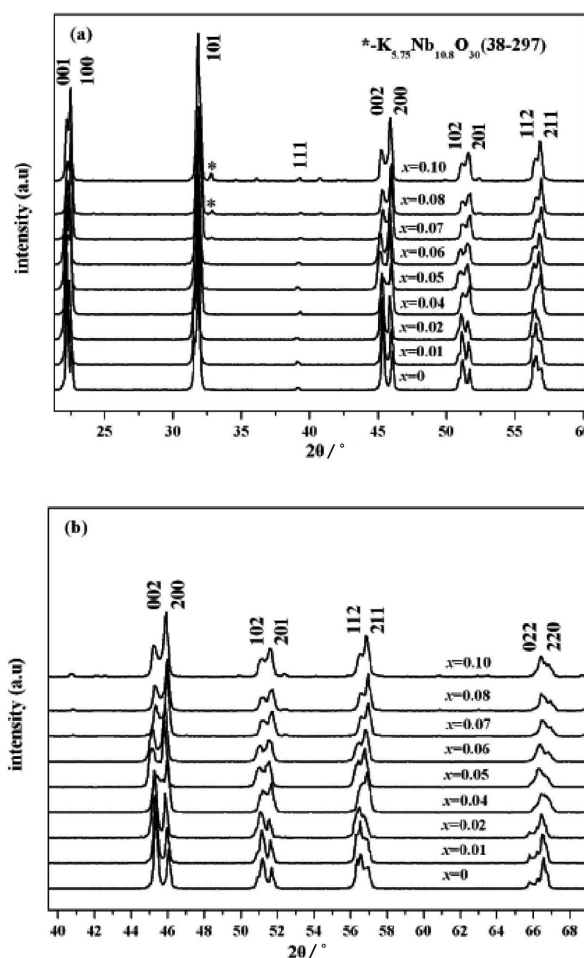


Fig. 1. XRD patterns of $(\text{K}_{0.52}\text{Na}_{0.48})_{1-x}\text{Li}_x(\text{Nb}_{1-x}\text{Sb}_x)\text{O}_3$ ceramics in the range of 2θ (a) from 20° to 60° and (b) from 40° to 68° .

[†] Contact author: Xiao Dingquan (D. Q. Xiao); E-mail: nic0402@scu.edu.cn

0.5/0.5 to 0.52/0.48, and Li and Sb were used as substitutes for (K, Na) and Nb, respectively. The effects of various amount of Li, Sb modified $\text{K}_{0.52}\text{Na}_{0.48}\text{NbO}_3$ lead-free piezoelectric ceramics were prepared by a conventional solid-state sintering process and their microstructure and electrical properties were investigated systematically.

2. Experimental procedure

K_2CO_3 (98%), Na_2CO_3 (99.8%), Li_2CO_3 (97%), Nb_2O_5 (99.5%), and Sb_2O_3 (99%) were used as raw materials to prepare $(\text{K}_{0.52}\text{Na}_{0.48})_{1-x}\text{Li}_x(\text{Nb}_{1-x}\text{Sb}_x)\text{O}_3$ ceramics ($x = 0, 0.01, 0.02, 0.04, 0.05, 0.06, 0.07, 0.08, \text{ and } 0.10$ respectively) by ordinary sintering. The stoichiometric mixture was ball milled for 24 h with zirconium ball media and alcohol, then dried and calcined at 850°C for 5 h. After that, the calcined powder was milled again for 12 h and pressed into disk of 13 mm in diameter and 1 mm in thickness under 6–8 MPa using PVA (10 mass%) as a binder. The green pellets, depending on their x , were sintered at $1040\text{--}1100^\circ\text{C}$ for

3 h in air. Silver electrodes were fired on the top and bottom surfaces of the samples. The ceramics were poled under a DC field of 3–4 kV/mm at 100°C in a silicone oil bath for 30 min.

X-ray diffract meter (DX-1000, Dandong, China) with $\text{Cu } K_\alpha$ radiation ($\lambda = 1.54184 \times 10^{-10}$ m) was utilized to identify the crystalline structure of the sintered samples. The microstructure of ceramics was observed by a scanning electron microscope (SEM) (S-450, Hitachi, Japan). The piezoelectric constant was measured using a piezo- d_{33} meter (ZJ-3A, China). The planar electromechanical coupling factor (k_p) was got by a resonance-anti resonance method through an impedance analyzer (HP 4194A) on the basis of IEEE standards. The polarization hysteresis loops were obtained with a Radiant Precision Workstation (USA) at room temperature.

3. Results and discussion

3.1 Phase development and microstructure

Figure 1 (a) shows the XRD patterns of $(\text{K}_{0.52}\text{Na}_{0.48})_{1-x}\text{Li}_x$

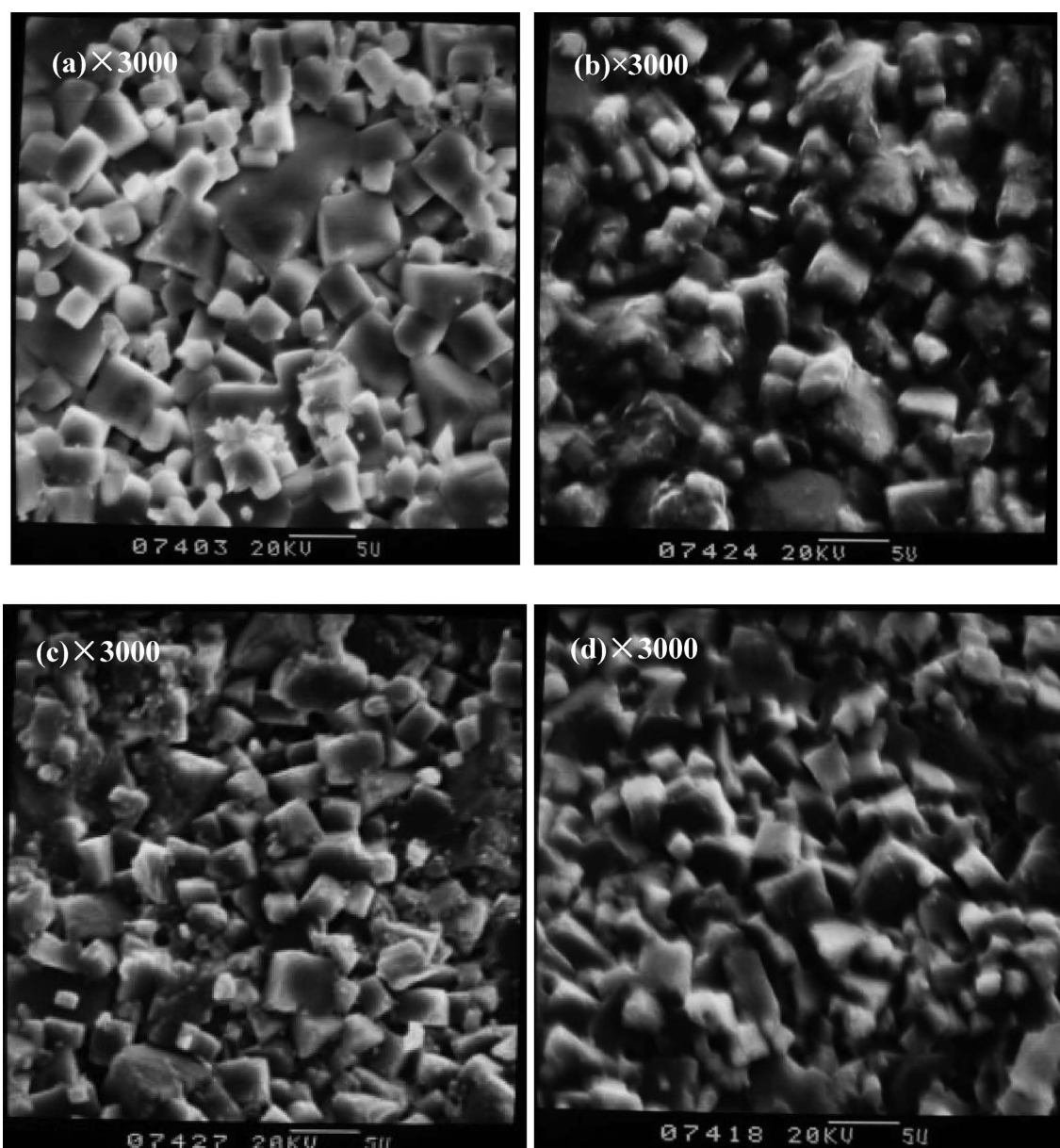


Fig. 2. SEM images of $(\text{K}_{0.52}\text{Na}_{0.48})_{1-x}\text{Li}_x(\text{Nb}_{1-x}\text{Sb}_x)\text{O}_3$ ceramics: (a) $x = 0$, (b) $x = 0.05$, (c) $x = 0.07$, and (d) $x = 0.08$.

(Nb_{1-x}Sb_x)O₃ ceramics with different x values. It is evident that the ceramics are of single perovskite phase as $0 \leq x \leq 0.07$. It is considered that Li⁺ and Sb⁵⁺ have entered into the (K_{0.52}Na_{0.48})⁺ and Nb⁵⁺ sites, respectively, to form a homogeneous solid solution. Nevertheless, some characteristic peaks of non-perovskite structure appear as $x = 0.08$, and the new phase presents in the system. Fig. 1 (b) is the magnified patterns of Fig. 1 (a) in the range of 2θ from 40° to 68° . It can be seen that the ceramic structure gradually changes with increasing x contents. As $0 \leq x \leq 0.02$, the ceramics are orthorhombic phase, and the ones are tetragonal phase as $0.06 \leq x \leq 0.08$. The orthorhombic and tetragonal phases of the samples coexisted in the composition range of $0.04 \leq x \leq 0.05$ at room temperature. It is also noted that the diffraction peak shifts slightly to lesser angle while $2\theta \sim 46.5^\circ$, and new phase peaks appear while $2\theta \sim 32.5^\circ$ as $x = 0.08$. This phenomenon is probably due to the geometrical distortion of the ceramics along with increasing the substitution of Li⁺ for (K_{0.52}Na_{0.48})⁺ and Sb⁵⁺ for Nb⁵⁺.

Figure 2 shows SEM images of (K_{0.52}Na_{0.48})_{1-x}Li_x(Nb_{1-x}Sb_x)O₃ ceramics as a function of x sintered at their optimum temperature. It is clear that this kind of ceramics with x being in the experimental range possess clear grain boundary and the crystallites size exhibits relatively homogeneous. As a result, dense microstructures of ceramics are formed.

3.2 Electrical properties

Figure 3 (a) and (b) show the dielectric and piezoelectric properties of (K_{0.52}Na_{0.48})_{1-x}Li_x(Nb_{1-x}Sb_x)O₃ ceramics as a function of the x respectively. It is obvious that d_{33} and k_p values enhance while $0 \leq x \leq 0.05$, and then the values slide down with

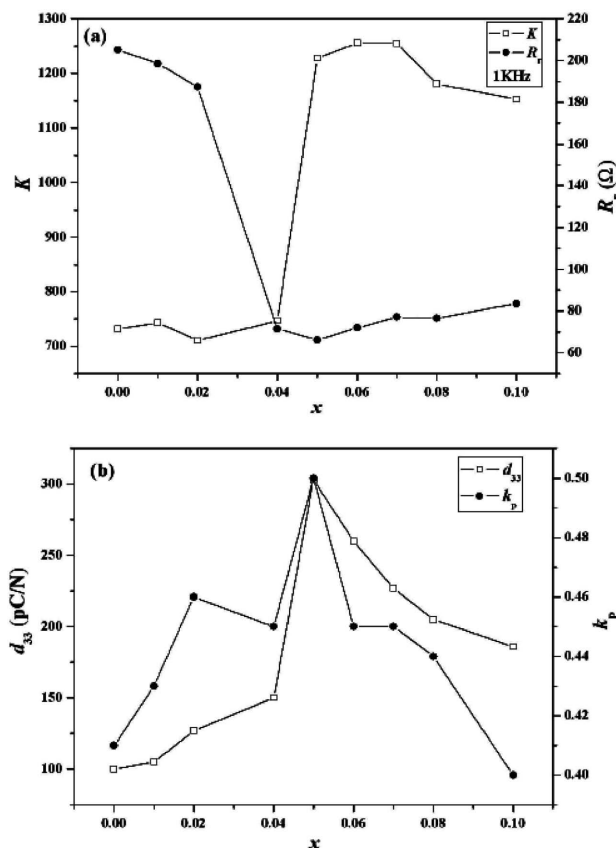


Fig. 3. Dielectric (a) and piezoelectric (b) properties of (K_{0.52}Na_{0.48})_{1-x}Li_x(Nb_{1-x}Sb_x)O₃ ceramics as a function of the x .

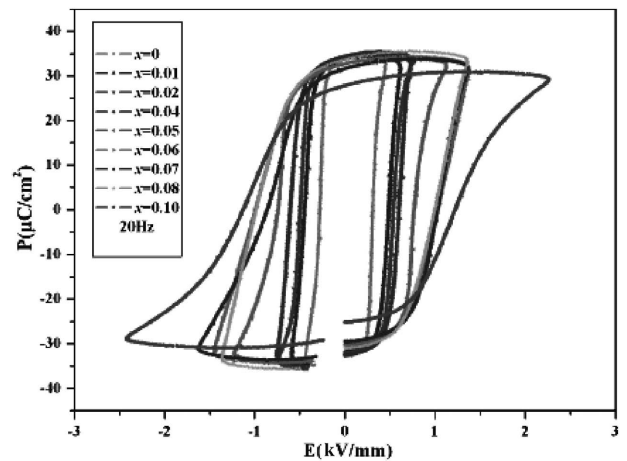


Fig. 4. P - E hysteresis loops of the (K_{0.52}Na_{0.48})_{1-x}Li_x(Nb_{1-x}Sb_x)O₃ ceramics measured at 20 Hz at room temperature.

x increases continuously. It is well known that buzzers application is one of the important applications of piezoelectric ceramics, and syntonc impedance (R_t) is the key parameter of buzzers. It is essential to reduce R_t values of KNN-based lead-free piezoelectric ceramics efficiently to commercial use. Therefore the value of syntonc impedance (R_t) of the ceramics were measured. The maximum values of d_{33} (303 pC/N) and k_p (0.50) of the ceramics appear at $x = 0.05$ [see Fig. 3(a)], while the relative dielectric constant (K) and syntonc impedance (R_t) give their values of 1228 and 66.1 Ω at $x = 0.05$ measured at 1 KHz [see Fig. 3(b)] respectively.

P - E hysteresis loops of the (K_{0.52}Na_{0.48})_{1-x}Li_x(Nb_{1-x}Sb_x)O₃ ceramics measured at 20 Hz at room temperature are showed in Fig. 4. It can be observed that the ceramics behave relatively better rectangle-like P - E loops. As shown in Fig. 4, the coercive field (E_c) gives its value of 0.310 kV/mm while $x = 0$, and increasing x value to 0.04 and 0.10, E_c value equals to 0.598 KV/mm and 1.224 kV/mm, respectively. Therefore, the coercive field (E_c) of the ceramics increases with x . Nevertheless, the remnant polarization (P_r) gives its value of 32.2 $\mu\text{C}/\text{cm}^2$, 31.8 $\mu\text{C}/\text{cm}^2$ and 26.8 $\mu\text{C}/\text{cm}^2$ while x value equals to 0, 0.04 and 0.10, respectively. Clearly, the remnant polarizations (P_r) of the ceramics show a bit reduce with x increasing. For the ceramics with the maximum values of d_{33} (303 pC/N) and k_p (0.50) when $x = 0.05$, the remnant polarization ($P_r = 31.2 \mu\text{C}/\text{cm}^2$) and coercive field ($E_c = 0.770$ kV/mm) values of the ceramics are also excellent.

4. Conclusions

(K_{0.52}Na_{0.48})_{1-x}Li_x(Nb_{1-x}Sb_x)O₃ lead-free piezoelectric ceramics have been prepared by a solid state reaction, their microstructure and electrical properties were characterized in detail. Clearly, the ceramics are of single perovskite phase as $0 \leq x \leq 0.07$, and the crystalline phases and microstructure of this kind of ceramics exhibited much dependence on the x content, and the orthorhombic and tetragonal phases of the samples coexisted in the composition range of $0.04 \leq x \leq 0.05$ at room temperature. The ceramic with $x = 0.05$ show the better die-, piezo- and ferroelectric properties: piezoelectric constant $d_{33} = 303$ pC/N, planar electromechanical coupling coefficient $k_p = 0.50$, the relative dielectric constant $K = 1228$, syntonc impedance $R_t = 66.1 \Omega$, remnant polarization $P_r = 31.2 \mu\text{C}/\text{cm}^2$, and coercive field $E_c = 0.770$ kV/mm. All of these results indicate that (K_{0.52}Na_{0.48})_{1-x}Li_x(Nb_{1-x}Sb_x)O₃ lead-free piezoelectric ceramics are promising

to practical applications.

Acknowledgement This work was supported by National Science Foundation of China (NSFC 50410179, 50572066, and 50772068) and Foundation of Doctor Training Program in University and College in China (Grant No. 20030610035).

References

- 1) E. Cross, *Nature*, **432**, 24–25 (2004).
- 2) Y. Satio, H. Takao, T. Tani, T. Nonoyama, K. Takatori, T. Homma, T. Nagaya and M. Nakamura, *Nature*, **432**, 84–87 (2004).
- 3) L. Egerton and D. M. Dillion, *J. Am. Ceram. Soc.*, **42**, 438–442 (1959).
- 4) R. E. Jaeger and L. Egerton, *J. Am. Ceram. Soc.*, **45**, 209–213 (1962).
- 5) Y. P. Guo, K. Kakimoto and H. Ohsato, *Appl. Phys. Lett.*, **85**, 4121–4123 (2004).
- 6) M. Matsubara, K. Kikuta and S. Hirano, *J. Appl. Phys.*, **97**, 114105, 1–7 (2005).
- 7) S. H. Park, C. W. Ahn, S. Nahm and J. S. Song, *Jpn. J. Appl. Phys.*, **43**, 8B, L1072–L1074 (2004).
- 8) D. J. Brooks, R. Brydson and R. E. Douthwaite, *Adv. Mater.*, **17**, 2474–2477 (2005).
- 9) P. Zhao, B. P. Zhang and J. F. Li, *Appl. Phys. Lett.*, **90**, 242909, 1–3 (2007).
- 10) R. Z. Zuo and C. Ye, *Appl. Phys. Lett.*, **91**, 062916, 1–3 (2007).
- 11) G. Z. Zang, J. F. Wang, H. C. Chen, W. B. Su, C. M. Wang, P. Qi, B. Q. Ming, J. Du and L. M. Zheng, *Appl. Phys. Lett.*, **88**, 212908, 1–3 (2006).
- 12) E. Hollenstein, M. Davis, D. Damjanovic and N. Setter, *Appl. Phys. Lett.*, **87**, 182905, 1–3 (2005).
- 13) Z. P. Yang, Y. F. Chang and L. L. Wei, *Appl. Phys. Lett.*, **90**, 042911, 1–3 (2007).
- 14) B. Q. Ming, J. F. Wang, P. Qi and G. Z. Zang, *J. Appl. Phys.*, **101**, 054103, 1–4 (2007).
- 15) Y. F. Chang, Z. P. Yang, Y. T. Hou, Z. H. Liu and Z. L. Wang, *Appl. Phys. Lett.*, **90**, 232905, 1–3 (2007).
- 16) G. Shirane, R. Newnham and R. Pepinsky, *Phys. Rev.*, **96**, 581–588 (1954).